

THE STRUCTURE EFFECTS IN POLARIZATION AND CROSS
SECTION IN INELASTIC $A(p, p')$ REACTION WITH THE ^{40}Ca
AND ^{12}C NUCLEI AT 1 GeV

O.V. Miklukho, A.Yu. Kisselev, G.M. Amalsky, V.A. Andreev,
G.E. Gavrilov, A.A. Izotov, N.G. Kozlenko, P.V. Kravchenko,
M.P. Levchenko, D.V. Novinskiy, A.N. Prokofiev, A.V. Shvedchikov,
S.I. Trush, A.A. Zhdanov

*B.P. Konstantinov Petersburg Nuclear Physics Institute, National Research
Centre Kurchatov Institute, Gatchina, 188300 Russia*

The polarization of the secondary protons in the inelastic (p, p') reaction on the ^{40}Ca and ^{12}C nuclei at the initial proton energy 1 GeV was measured in a wide range of the scattered proton momenta at a laboratory angle $\Theta=21^\circ$. The cross sections of the reaction were measured as well. The outgoing protons from the reaction were detected using a magnetic spectrometer equipped with a multiwire-proportional chambers polarimeter. A structure in the polarization and cross section data, related probably to scattering off the nucleon correlations in the nuclei, was observed.

PACS numbers: 13.85.Hd, 24.70.+s, 25.40.Ep, 29.30.-h

Comments: 13 pages, 5 figures, 7 tables.

Category: Nuclear Experiment (nucl-ex)

1 Introduction

—This work is a part of the experimental program in the framework of which the effects of nucleon clusterization in nuclear matter is studied at the PNPI synchrocyclotron with the 1 GeV proton beam [1, 2]. Earlier, in the first inclusive experiment, the scattered proton polarization in the reaction $^{40}\text{Ca}(p, p')\text{X}$ at $\Theta=21^\circ$ was measured [1]. At a proper secondary proton momentum, when scattering off the ^4He -like nucleon cluster (nucleon correlation (NC)) in the ^{40}Ca nucleus could dominate, the measured polarization was found to be close to that in the free elastic proton- ^4He scattering. We investigated in details the polarization in the reaction and observed a structure in the experimental data [2]. The latter could be related to scattering off the multi-nucleon correlations in the nucleus [3, 4].

In this paper we present the results of the experiment, in which two inclusive reactions $^{40}\text{Ca}(p, p')\text{X}$ and $^{12}\text{Ca}(p, p')\text{X}$ at the scattering angle of the secondary protons $\Theta=21^\circ$ were investigated. In this experiment, besides the polarization of the final protons, we also measured the differential cross section of the reactions. These measurements were performed in a wide range of the scattered proton momentum K ($K = 1370\div 1670$ MeV/c). Note that the momentum corresponding to a maximum of the quasielastic pN peak is close to 1480 MeV/c. The data were obtained in narrow momentum intervals ($\simeq 10$ MeV/c) and with a small gap between the intervals ($\simeq 10$ MeV/c). Of a special interest was to make the measurements at the $K > 1530$ MeV/c up to the momentum corresponding to the excited level of the nucleus under investigation. In this region, since the NC are more massive than nucleons, the quasi-elastic (p, p' NC) reactions (the elastic scattering off the NC in nuclear medium) are kinematically preferable. At $K > 1580$ MeV/c the scattering off the independent (uncorrelated) nuclear nucleons is strongly suppressed, since they have a minimal momentum larger than the Fermi momentum K_F (≈ 250 MeV/c) [2].

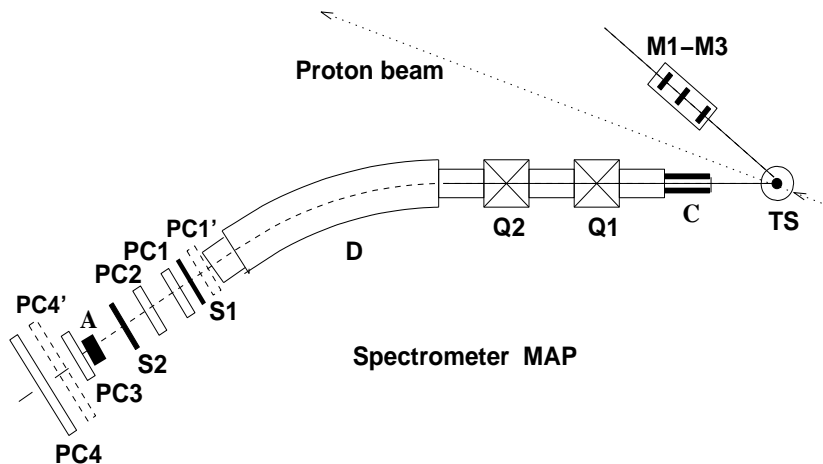


Figure 1: The experimental setup. TS is the target of the MAP spectrometer; Q1÷Q2 are the magnetic quadrupoles; D is the dipole magnet; C1 is the collimator; S1÷S2 and M1÷M3 are the scintillation counters; PC1÷PC4, PC1', PC4' and A are the proportional chambers and the carbon analyzer of the MAP polarimeter, respectively.

Table 1: Target parameters

Target	Dimensions, mm thickness x width x height	Isotope concentration, %	Density, g/cm ³
CH ₂	4 x 15 x 70		1.0
C	4 x 15 x 70	98.9	1.6
CH ₂ foil	0.1 x 4 x 10		1.0
¹² C	4 x 7 x 10	98.9	1.6
⁴⁰ Ca	4 x 7 x 10	97.0	1.55

The general layout of the experimental setup is presented in Fig. 1.

2 Experimental method

The proton beam of the PNPI synchrocyclotron was focused onto the target TS of the magnetic spectrometer MAP. The beam intensity was monitored by the scintillation telescope M1, M2, M3. The diameter of the beam spot on the target was $\simeq 25$ mm. Large CH₂ and C targets, CH₂ foils for the setup calibration, and small ¹²C and ⁴⁰Ca targets for the main measurements were used in the experiment (Table 1).

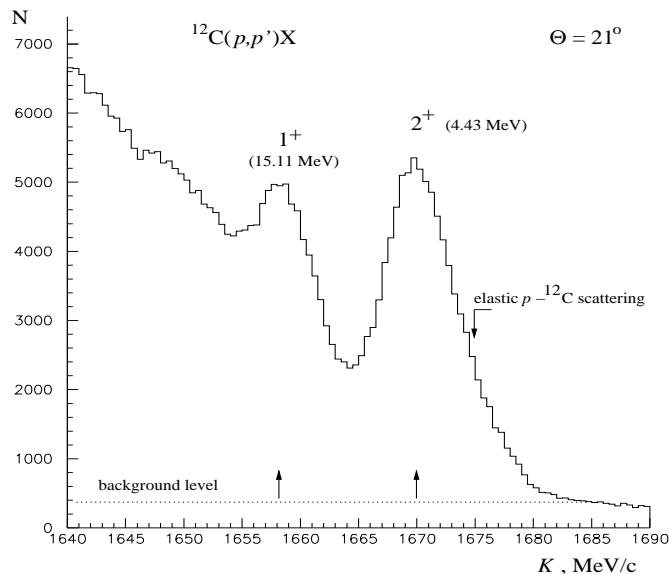


Figure 2: Momentum distribution in the inclusive reaction $^{12}\text{C}(p,p')\text{X}$ at a scattering angle $\Theta=21^\circ$.

The spectrometer was used to measure the momenta of the secondary protons from the inclusive (p, p') reaction as well as their polarization. The momentum of the proton was determined using the coordinate information from the proportional chambers PC1-X and PC2-X. The momentum resolution of the spectrometer in this experiment was $\pm 2.5 \text{ MeV}/c$. This value was estimated by measuring the width of the clearly separated 2^+ excited level in the (p, p') reaction with the ^{12}C nucleus at the scattering angle 21° under investigation (Fig. 2). In Fig. 2 we also observed a peak which can be identified as the 1^+ excited level predicted in [5].

The polarization of the final protons was found from an azimuthal asymmetry of the proton scattering off the carbon analyzer A, using the track information from the proportional chambers (PC1÷P4 and PC1', PC4') of the polarimeter [6]. The average analyzing power of the polarimeter was calculated using the parametrization $A(K, \theta_s)$ from [7].

The main parameters of the MAP spectrometer and the polarimeter are listed in Tables 2 and 3, respectively.

The calibration of the analyzing power of the polarimeter was carried out using the pp elastic scattering polarization data obtained in this experiment. For the calibration in a wide range of the secondary proton energy we performed the polarization measurements with the polyethylene and carbon targets (the large CH_2 and C targets, Table 1) at different angular ($\Theta = 13.5^\circ \div 23^\circ$) and proper momentum settings of the spectrometer. The observed values of the pp polarization were compared with the predictions in the framework of the phase-shift

Table 2: Parameters of the magnetic spectrometer

Maximum particle momentum, [GeV/c]	1.7
Horizontal angle acceptance $\Delta\Theta_H$, [deg]	0.8
Vertical angle acceptance $\Delta\Theta_V$, [deg]	1.9
Solid angle acceptance Ω , [sr]	$4.0 \cdot 10^{-4}$
Momentum acceptance $\Delta K/K$, [%]	8.0
Dispersion in the focal plane D_f , [mm/%]	22.0
Momentum resolution (FWHM), [MeV/c]	~ 5.5

Table 3: Polarimeter parameters

Carbon block thickness, [mm]	155
Polar angular range, [deg]	$3 \div 16$
Average analyzing power	≥ 0.2
Efficiency, [%]	~ 5

analysis [8] and a correction for the analyzing power of the polarimeter has been done. The uncertainty of the calibration was included in the total error of the polarization measurement.

The relative differential cross section of the reactions $\sigma^{incl} = \frac{d^2\sigma}{d\Omega dK}$ was found from the momentum spectra obtained at different momentum settings of the spectrometer. The monitor number and efficiency of the proportional chamber PC2-X for each momentum setting were taken into account. To subtract a background, the measurements with an empty target and with the 100 μm tungsten string supports of a target were done. An absolute normalization of the cross section in the reaction with the ^{12}C nucleus was made with the large CH_2 target (Table 1) in a momentum range near the quasi-elastic scattering peak maximum. The cross section in the pp elastic scattering was calculated in the framework of the phase-shift analysis [8]. At the scattering angle $\Theta = 21^\circ$ a value of 2.92 mb/sr (in the centre-of-mass system) was obtained. To make this normalization for the reaction with the ^{40}Ca nucleus, we made the measurements with the ^{40}Ca target, with the ^{40}Ca target + additional target CH_2 -foil (Table 1), and again with the ^{40}Ca target. These data allowed us to estimate the admixture of hydrogen in the superficial layer of the ^{40}Ca target. The relative systematic errors $\delta\sigma^{incl}/\sigma^{incl}$ of the cross section (σ^{incl}) normalization for the reactions $^{12}\text{C}(p, p')\text{X}$ and $^{40}\text{Ca}(p, p')\text{X}$ were $\pm 1.5\%$ and $\pm 3.5\%$, respectively. An uncertainty of the cross section calculations in the elastic pp scattering [8] was not included.

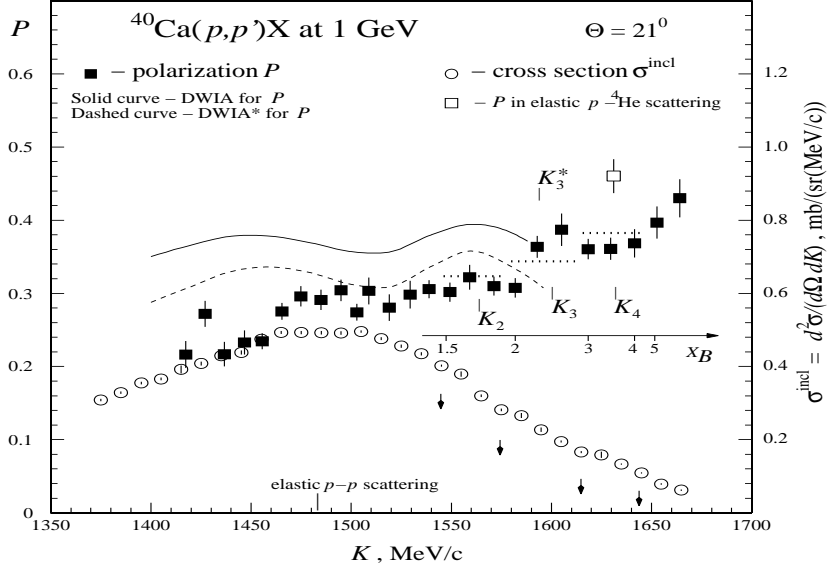


Figure 3: Polarization P of the protons scattered at an angle $\Theta = 21^\circ$ (black squares) in the inclusive reaction $^{40}\text{Ca}(p, p')X$ versus the secondary proton momentum K . The circles correspond to the differential cross sections $\frac{d^2\sigma}{d\Omega dK}$ measured in the reaction. Solid and dashed curves are a result of the polarization calculations in the framework of the DWIA and DWIA*, respectively. The empty square corresponds to the polarization in the elastic $p-^4\text{He}$ scattering [9]. The dotted lines cover the K intervals II, III, IV and the Bjorken variable scale are defined in the text.

3 Experimental results and discussion

In Fig. 3 and Fig. 4 the measured polarizations P (black squares) and cross sections $\frac{d^2\sigma}{d\Omega dK}$ (circles) in the reactions $^{40}\text{Ca}(p, p')X$ and $^{12}\text{C}(p, p')X$ are plotted versus the scattered proton momentum K . Small errors of the cross section measurements are presented inside the circles. The experimental data are also given in Tables 4÷7. The empty square corresponds to an estimate of the polarization in the elastic $p-^4\text{He}$ scattering [9]. The solid curve in Fig. 3 presents the polarization calculated in the framework of a spin-dependent Distorted Wave Impulse Approximation (DWIA) [10]. The dashed curves in Fig. 3 and Fig. 4 are the result of the calculations in the framework of the DWIA taking into account the relativistic distortion of the nucleon spinor in nuclear medium (DWIA*) [10, 11]. In this approach the proton scattering off the independent nuclear nucleons was taken into account only. The calculations were performed using the THREEDEE code [12].

As seen from Figs. 3, 4 in the region of the $K > 1530$ MeV/c a drop of the cross section slows down at the momenta close to these marked by arrows. The momentum intervals between the adjacent arrows are indicated in the figures as the dotted line segments in an area of the polarization data. Let us denote these

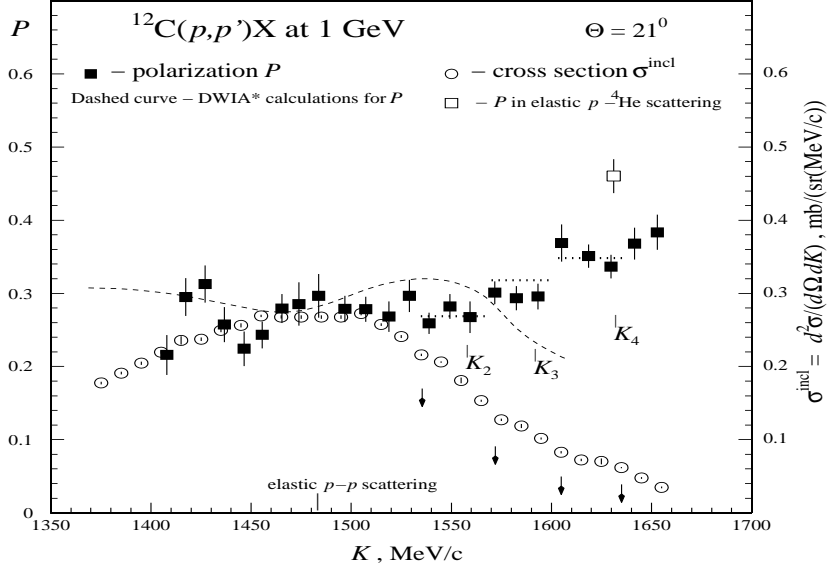


Figure 4: Polarization P of the protons scattered at an angle $\Theta = 21^\circ$ (black squares) in the inclusive reaction $^{12}\text{Ca}(p, p')X$ versus the secondary proton momentum K . The circles correspond to the differential cross sections $\frac{d^2\sigma}{d\Omega dK}$ measured in the reaction. Dashed curve is a result of the polarization calculations in the framework of the DWIA*. The empty square corresponds to the polarization in the elastic p - ^4He scattering [9]. The dotted lines cover the K intervals II, III, and IV, defined in the text.

momentum ranges as II, III, and IV in the direction of momentum growth. Note that the onset of each momentum interval (II, III, and IV) for the ^{40}Ca nucleus is shifted with respect to that for the ^{12}C nucleus by $\sim 5\div 10$ MeV/c towards higher values. The value of the polarization in the momentum ranges is practically constant excluding the interval III for the ^{40}Ca data. The polarization increases from the interval II to interval IV. At momenta $K > 1580$ MeV/c the large values of the polarization and cross section [2] can not be explained only by the proton scattering off the uncorrelated nuclear nucleons. Possible, such behaviour of polarization and cross section in the momentum ranges II, III, and IV can be related to a proton quasielastic scattering off the two-nucleon, three-nucleon, and four-nucleon correlations. The value of the polarization in the proton interaction with a NC can depend on the number and isospin properties of nucleons in the correlation. According to [13], larger values of the secondary proton polarization can be observed in the elastic scattering off a light nucleus in comparison with that in the scattering off independent nuclear nucleons.

The calculated final proton momenta K_2 , K_3 (K_3^*), and K_4 corresponding to the maxima of the quasi-elastic peaks in the $^{40}\text{Ca}(p, p' \text{NC})X$ and $^{12}\text{C}(p, p' \text{NC})X$ reactions on the stationary NC consisting of two, three, and four nucleons are shown in Figs. 3, 4. In these calculations the masses of real light nuclei with simple structure ^2H , ^3He (^3H), and ^4He were used as the NC masses. The resid-

ual nuclei (X) in the reactions were assumed to be in a ground state. As seen in Fig. 3 the momenta K_2 (1563 MeV/c), K_3 (1599 MeV/c), K_3^* (1593 MeV/c), and K_4 (1631 MeV/c), and in Fig. 4 the momenta K_2 (1557 MeV/c), $K_3 \approx K_3^*$ (1591 MeV/c), and K_4 (1631 MeV/c) are within the momentum intervals II, III, and IV, respectively. This observation stays true if the NC masses were smaller (due to the nuclear medium modification [11]) than the mass of the corresponding free light nucleus. A $\sim 10\%$ decrease of the NC masses reduces the values of the momenta K_2 , K_3 (K_3^*), and K_4 by ~ 12 MeV/c, ~ 8 MeV/c, and ~ 6 MeV/c, respectively. Note here that a high momentum range, just following the momentum interval IV, possibly corresponds to quasi-elastic scattering off the residual nuclei X of the reactions considered above.

The DWIA* calculations show that the contribution from the quasi-elastic scattering off the uncorrelated nucleons in the momentum interval II is rather large [2]. At $K > 1580$ MeV/c, including the momentum intervals III and IV, this contribution is essentially suppressed since the nuclear nucleons have momenta higher than the Fermi momentum $k_F \approx 250$ MeV/c. The polarizations measured in the momentum interval IV (P_{IV}) in the scattering off the ^{40}Ca and ^{12}C nuclei (see Figs. 3, 4) are practically the same ($P_{IV}(\text{Ca}) = 0.363 \pm 0.009$ and $P_{IV}(\text{C}) = 0.348 \pm 0.010$). The polarization P_{IV} is less than that ($P_{4\text{He}}$) in the free elastic p - ^4He scattering (empty square) [9]. This can be related to a modification of proton interaction with the four-nucleon cluster in nuclear medium [6]. The relative difference of these polarizations $(P_{4\text{He}} - P_{IV})/P_{4\text{He}} \sim 0.2$ is close to that of the polarizations (P_{DWIA^*} and P_{DWIA}) calculated in the DWIA* and DWIA approximations (Fig. 3) for the quasi-elastic scattering off the uncorrelated nucleons $(P_{DWIA} - P_{DWIA^*})/P_{DWIA} \sim 0.15$ at $K \approx 1580$ MeV/c.

The widths (ΔK) of the momentum intervals II \div IV are not determined by the horizontal angular acceptance of the spectrometer alone ($\Delta\Theta_h \sim 1^\circ$). The main contribution to the ΔK can come from a motion of the NC in the nucleus. For instance, if the scattering occur off the four-nucleon correlations at rest in the nucleus then the ΔK width of the momentum interval IV would be equal to ~ 5.5 MeV/c. This value is about 4.5 times less than that estimated from this experiment $\Delta K \sim 25$ MeV/c. So, due to a motion of the NC, the effective angular acceptance essentially increases ($\Delta\Theta_h \sim 4.5^\circ$). This enables us to observe the polarization angular distribution in scattering from the NC within the momentum interval IV. In Fig. 5 the polarization angular distribution measured in the free elastic p - ^4He scattering is shown [9]. The dotted line segment corresponds to the effective angular acceptance seen in the inclusive reaction in the momentum interval IV. According to the data in the figure, we can expect that the polarization momentum dependence in the proton scattering off the four-nucleon correlations in the nuclei can also be close to uniform. A growth of the polarization in the momentum interval III in the scattering off the ^{40}Ca nucleus (Fig. 3) is possibly related to that the momentum regions of scattering off the ^3He - and ^3H -like correlations overlap only partially. This follows from a noticeable difference of the

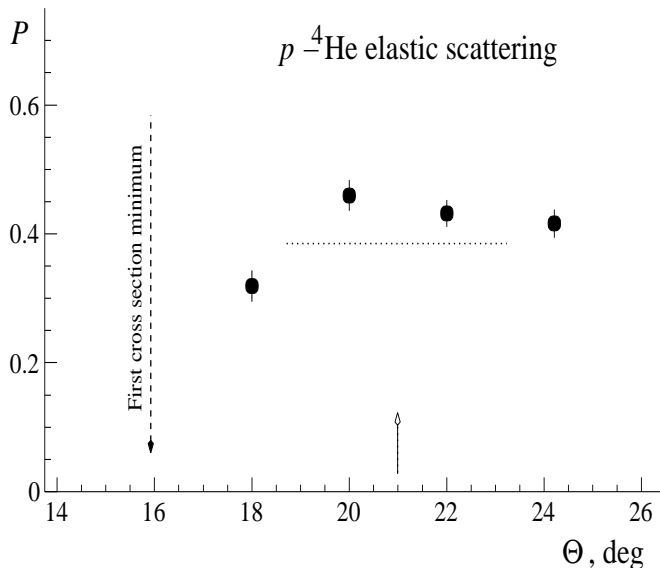


Figure 5: Angular dependence of the polarization in the elastic p - ${}^4\text{He}$ scattering at 1 GeV [9]. The dotted line covers the effective angular acceptance observed in the inclusive (p, p') reaction.

momenta K_3 and K_3^* mentioned above, being $K_3 > K_3^*$ (for the ${}^{12}\text{C}$ data these momenta are almost the same). We suppose that the polarization in the elastic scattering off the ${}^3\text{He}$ nucleus is essentially larger than that off the ${}^3\text{H}$ nucleus. So, at momenta close to the end of the interval III, the polarization is possibly determined by the scattering off the ${}^3\text{He}$ -like correlations. At $K < K_3^*$ the processes of scattering off these three-nucleon correlations are mixed. For reliable verification of the above supposition, the polarization calculations in the framework of the Glauber's multiple nucleon-nucleon scattering theory [14] should be done. We were only based on the fact that at the initial proton energy 1 GeV the polarization in the elastic scattering off neutron is about 25 % less than that in the proton-proton scattering, and the number of neutrons in ${}^3\text{He}$ is smaller than in the ${}^3\text{H}$ nucleus.

We would like to make some remarks about measured results in the momentum range $1420 \text{ MeV}/c < K < 1530 \text{ MeV}/c$ (denote this range as I) covering the momentum ($K \sim 1480 \text{ MeV}/c$) corresponding to a maximum of the pN quasi-elastic peak (see Figs. 3, 4). In the range I, where the cross section of the inclusive (p, p') reaction has large values and depends smoothly on the K , a contribution from the multi-step processes of knocking out nucleons from a nucleus, can be noticeable [15]. The outgoing proton momentum in these processes decreases as compared with that in the one-step (p, p') reaction under investigation. Due to this effect a shape of the quasi-elastic peak can be distorted. It is important to note here, in the momentum region $K > 1530 \text{ MeV}/c$, where the cross section dips rapidly with a growth of the K , the multi-step processes are essentially unable

to distort the momentum distribution measured in the reaction. The DWIA* predictions of the outgoing proton polarization for the reaction $^{12}\text{C}(p, p')X$ (Fig. 4) are in a good consent with the experimental data in a narrow region around the momentum $K \sim 1480$ MeV/c. The variation of the measured polarization in the range I is apparently a combined effect of the multi-step reactions and a discrete energy-shell structure of the ^{12}C nucleus.

Last we make a comment on the kinematics of the present (p, p') experiment. In the momentum range $1480 \div 1650$ MeV/c the value of the transferred four-momentum Q stays almost constant and is equal to ≈ 600 MeV/c. The latter value is about two times higher than that of the Fermi momentum. So, the Bjorken kinematical variable $x_B = \frac{Q^2}{2m\nu}$ is only determined by the energy transfer ν (where m is nucleon mass). In Fig. 3, there is an additional horizontal scale for x_B indicated. As seen from the figure, for the reaction with the ^{40}Ca nucleus the momentum intervals II, III, and IV correspond to the x_B intervals $1.5 < x_B < 2$, $2 < x_B < 3$, and $3 < x_B < 4$, respectively. Due to the above mentioned difference in the momentum interval onsets for the ^{12}C and ^{40}Ca nuclei (it is possible related to a large mass difference of the nuclei), the corresponding x_B intervals in the reaction $^{12}\text{C}(p, p')X$ are $1.4 < x_B < 1.8$, $1.8 < x_B < 2.5$, and $2.5 < x_B < 3.7$. It is interesting to note that in the JLAB unpolarized (e, e') experiment at $E_e \sim 4.6$ GeV and $Q^2 > 1.4$ GeV $^2/c^2$, the effects from the two-nucleon and three-nucleon correlations in the cross section were observed in the x_B ranges $1.5 < x_B < 2$ and $2.25 < x_B < 2.8$, respectively [4].

4 Summary

The polarization of the secondary protons in the inelastic (p, p') reaction with the ^{40}Ca and ^{12}C nuclei and the cross section of these reactions were investigated at the 1 GeV initial proton energy and the scattering angle $\Theta = 21^\circ$. The data were obtained in a wide range of the scattered proton momentum K covering the pN quasi-elastic peak and a high momentum region ($K > 1530$ MeV/c) up to the momentum corresponding to the excited levels of the nucleus under investigation. The measurements were done in narrow momentum intervals ($\simeq 10$ MeV/c) and with a small gap between the intervals ($\simeq 10$ MeV/c).

A polarization growth with the final state proton momentum at $K > 1530$ MeV/c was found. A structure in the polarization and cross section data in this region was observed for the first time. The structure is possibly related to a proton quasielastic scattering off the two-nucleon, three-nucleon, and four-nucleon correlations.

The authors are grateful to the PNPI 1 GeV proton accelerator staff for the stable beam operation. Also, the authors would like to express their gratitude to A.A. Vorobyov and S.L. Belostotski for their support and fruitful discussions. We thank D.A. Prokofiev for his valuable help in this paper preparation.

Table 4: The polarization P of the scattered proton in the reaction $^{40}\text{Ca}(p, p')X$ at 1 GeV and lab. angle $\Theta=21^\circ$

K MeV/c	P	K MeV/c	P	K MeV/c	P
1417.3	0.217±0.018	1502.8	0.274±0.011	1592.9	0.364±0.015
1427.0	0.272±0.018	1508.8	0.303±0.019	1605.1	0.387±0.022
1436.7	0.217±0.017	1519.1	0.281±0.018	1618.4	0.361±0.014
1446.6	0.233±0.017	1529.4	0.298±0.019	1629.6	0.361±0.015
1455.5	0.234±0.011	1538.9	0.306±0.013	1641.6	0.368±0.019
1465.4	0.275±0.012	1549.3	0.302±0.013	1652.7	0.397±0.022
1474.8	0.296±0.014	1559.1	0.322±0.017	1664.0	0.430±0.026
1484.8	0.291±0.014	1571.3	0.310±0.013		
1495.0	0.304±0.015	1582.0	0.308±0.013		

Table 5: The polarization P of the scattered proton in the reaction $^{12}\text{C}(p, p')X$ at 1 GeV and lab. angle $\Theta=21^\circ$

K MeV/c	P	K MeV/c	P	K MeV/c	P
1407.9	0.216±0.027	1483.8	0.297±0.030	1571.6	0.301±0.015
1417.4	0.295±0.026	1496.9	0.279±0.018	1582.4	0.294±0.017
1427.0	0.313±0.025	1507.3	0.278±0.017	1593.3	0.296±0.018
1436.7	0.257±0.024	1518.8	0.268±0.021	1605.1	0.369±0.025
1446.5	0.224±0.024	1529.1	0.297±0.022	1618.5	0.351±0.016
1455.5	0.243±0.018	1538.9	0.259±0.015	1629.7	0.337±0.016
1465.3	0.279±0.020	1549.3	0.282±0.017	1641.6	0.368±0.022
1473.8	0.285±0.030	1559.3	0.267±0.022	1652.9	0.384±0.024

Table 6: The cross section of the reaction $^{40}\text{Ca}(p, p')\text{X}$ at 1 GeV and lab. angle $\Theta=21^\circ$

K MeV/c	$\frac{d^2\sigma}{d\Omega dK}$ mb/(sr·MeV/c)	K MeV/c	$\frac{d^2\sigma}{d\Omega dK}$ mb/(sr·MeV/c)	K MeV/c	$\frac{d^2\sigma}{d\Omega dK}$ mb/(sr·MeV/c)
1375.0	.3085±.0032	1475.1	.4928±.0047	1574.9	.2814±.0036
1385.0	.3283±.0034	1485.0	.4922±.0049	1584.9	.2659±.0070
1395.1	.3547±.0034	1495.0	.4918±.0047	1594.9	.2271±.0060
1405.1	.3659±.0038	1505.0	.4956±.0029	1604.9	.1950±.0028
1415.0	.3921±.0107	1515.0	.4760±.0040	1614.9	.1660±.0028
1425.0	.4083±.0051	1525.0	.4560±.0043	1625.0	.1585±.0082
1435.1	.4294±.0053	1535.0	.4347±.0043	1634.9	.1331±.0015
1445.1	.4385±.0055	1545.0	.4023±.0025	1644.9	.1090±.0015
1455.1	.4750±.0034	1554.9	.3793±.0076	1654.9	.0788±.0021
1465.1	.4932±.0043	1565.0	.3197±.0036	1664.9	.0622±.0019

Table 7: The cross section of the reaction $^{12}\text{C}(p, p')\text{X}$ at 1 GeV and lab. angle $\Theta=21^\circ$

K MeV/c	$\frac{d^2\sigma}{d\Omega dK}$ mb/(sr·MeV/c)	K MeV/c	$\frac{d^2\sigma}{d\Omega dK}$ mb/(sr·MeV/c)	K MeV/c	$\frac{d^2\sigma}{d\Omega dK}$ mb/(sr·MeV/c)
1375.1	.1774±.0018	1475.0	.2677±.0024	1574.9	.1272±.0016
1385.1	.1911±.0020	1485.0	.2676±.0025	1584.9	.1186±.0029
1395.1	.2045±.0021	1495.0	.2676±.0024	1594.9	.1016±.0013
1405.0	.2197±.0023	1505.0	.2723±.0023	1604.9	.0829±.0017
1415.0	.2357±.0056	1515.0	.2573±.0018	1614.9	.0722±.0017
1425.0	.2373±.0025	1525.0	.2410±.0019	1624.9	.0703±.0041
1435.0	.2494±.0026	1535.0	.2159±.0017	1635.0	.0618±.0009
1445.0	.2562±.0028	1544.9	.2061±.0011	1644.9	.0476±.0011
1455.0	.2692±.0017	1554.9	.1810±.0037	1655.0	.0349±.0012
1465.0	.2677±.0023	1564.9	.1533±.0015		

References

- [1] O. V. Miklukho, G. M. Amalsky, V. A. Andreev et al., arXiv:1103.6113v1 [nucl-ex] (2011).
- [2] O. V. Miklukho, A. Yu. Kisselev, G. M. Amalsky et al., JETP Letters **102**, 11 (2015).
- [3] D. I. Blokhintsev, Zh. Eksp. Teor. Fiz. **33**, 1295 (1957).
- [4] K. S. Egiyan et al., Phys. Rev. Lett. **96**, 082501 (2006).
- [5] R. D. Viollier, ANNALS OF PHYSICS **93**, 335 (1975).
- [6] O. V. Miklukho, A. Yu. Kisselev, D. A. Aksenov et al., Phys. Atom. Nucl. **76**, 871 (2013).
- [7] O. Ya. Fedorov, Preprint LNPI-484 (Gatchina, 1979) [in Russian].
- [8] J. Bystricky, F. Lehar, and P. Winternitz, J. Phys. (Paris) **39**, 1 (1978).
- [9] O. V. Miklukho, G. M. Amalsky, V. A. Andreev et al., Yad. Fiz. **69**, 474 (2006) [Phys. Atom. Nucl. **69**, 452 (2006)].
- [10] V. A. Andreev, M. N. Andronenko, G. M. Amalsky et al., Phys. Rev. C **69**, 024604 (2004).
- [11] C. J. Horowitz and M. J. Iqbal, Phys. Rev. C **33**, 2059 (1986).
- [12] N. S. Chant and P. G. Roos, Phys. Rev. C **27**, 1060 (1983).
- [13] H. Faissner, *Polarisierte Nucleonen I: Polarisation durch streuung* (Springer, 1959).
- [14] R. J. Glauber, *Lectures in Theoretical Physics*, eds. W. E. Brittin et al., **1**, 315 (Interscience, New York, 1959).
- [15] R. D. Smith and S. J. Wallace, Phys.Rev. C **32**, 1654 (1985).